THE PENNSYLVANIA STATE UNIVERSITY
SCHREYER HONORS COLLEGE

DEPARTMENT OF MECHANICAL ENGINEERING

EFFECT OF REYNOLDS NUMBER ON MECHANICS OF WATER BOATMAN LOCOMOTION

REBECCA DENBY
SPRING 2019

A thesis
submitted in partial fulfillment
of the requirements
for a baccalaureate degree
in Mechanical Engineering
with honors in Mechanical Engineering

Reviewed and approved* by the following:

Margaret L. Byron
Assistant Professor of Mechanical Engineering
Thesis Supervisor

Stephanie Stockar
Assistant Professor of Mechanical Engineering
Honors Adviser

* Signatures are on file in the Schreyer Honors College.

ABSTRACT

Understanding the hydrodynamics of swimming requires an understanding of the forces involved in propulsion through a fluid. At the centimeter-scale at which many freshwater invertebrates operate, these fluid forces are not well understood. We seek to better understand the hydrodynamics and kinematics of swimming in these animals, as locomotion is crucial to survival, especially for keystone species living in sensitive ecosystems. At the length and velocity scales at which these animals operate, intermediate Reynolds numbers imply that both inertia and viscosity are important for propulsion. One group of insects that falls into the intermediate Reynolds number regime is the family Corixidae, known as the water boatmen. To gain a better understanding of the propulsive forces dominating the locomotion of the boatman, this study investigates kinematics of the power and recovery strokes using high speed cinematography. This study also explores the morphology of hairy appendages and identifies the contributions to propulsion by area changes experienced by the appendage. Furthermore, this study aims to understand possible biological implications of observed behaviors.

TABLE OF CONTENTS

NOMENCLATURE

A = paddle area

d = setae diameter

D = intersetal spacing

l_1 = major length of paddle

l_2 = metatarsal width

l_3 = minor length of paddle

L = hind limb length

N = number of frames

Re = Reynolds number

Re_s = Reynolds number of setae

u = tangential velocity

α = angle of attack of hind limb

θ = angle of setae

ν = kinematic viscosity

ω = angular velocity

LIST OF FIGURES

LIST OF TABLES

ACKNOWLEDGEMENTS

I would like to express my thanks to my research advisor, Dr. Margaret Byron, and the students of the Environmental and Biological Fluid Mechanics Lab for giving their time and effort to teach me a variety of research skills. Thank you for being available and willing to share your knowledge on research techniques and never failing to answer my questions regarding the research experience. Thank you to Timothy Stecko and Whitney Yetter at the Center for Quantitative Imaging for providing knowledge and expertise on the Micro-CT scanner and scanning techniques and to the Energy and Environmental Sustainability Laboratory for providing funding to make use of this technology possible. I would also like to thank Gail Denby and Rick Denby for their never-ending support throughout my pursuit of an honors undergraduate degree.

Chapter 1

Introduction

Motion through a fluid is governed by both viscous and inertial forces. The Reynolds number (Re) for a given scale and velocity represents the ratio of these forces, providing an indication to which of the two will dominate the motion. Larger animals (e.g. >10 cm) moving at higher velocities (e.g. >1 m/s) will produce thrust dominated by inertial forces, thus having higher Re (Re>>1) (Jordan, 1992), (Lighthill, 1969). Similarly, a smaller animal (e.g. < 1 mm) moving at a lower velocity (e.g. <1 cm/s) will have a lower Re (Re<<1), indicating that viscous forces dominate (Godoy-Diana & Thiria, 2018; Jordan, 1992; Purcell, 1977). However, for aquatic animals of lengths between one millimeter to one centimeter and swimming at typical speeds, Re will often fall between $1 < Re < 1000$. This range is considered intermediate (neither high nor low). In this region, both inertial and viscous forces play a role in propulsion through a fluid medium (Childress, 1981).

A swimming animal must overcome a combination of skin friction (dominant at low Re) and/or pressure drag (dominant at high Re) by generating thrust. At low Re, enough thrust must be generated to overcome the viscous forces that dominate in this regime. As an animal moves through water, an opposition caused by the viscous shearing of the fluid will result in skin friction (Godoy-Diana & Thiria, 2018); pressure drag is negligible in these highly viscous flows. At high Re, thrust must overcome the pressure drag that results from separations between the surface and velocity streamlines (Fish & Lauder, 2006); viscous drag is usually neglected, as it is

small compared to the pressure drag. At intermediate Re, neither viscous nor pressure drag may be neglected; both forces contribute to overall drag and therefore increase the required thrust.

One group of aquatic animals that operates in the intermediate Re regime is the family Corixidae, known as the water boatman. Approximately one centimeter in length, the boatman is a flat-bodied insect typically marked with a yellow and brown pattern on its back (Hungerford, 1919). The boatman is a rowing insect that occupies freshwater bodies that contain organic matter for feeding (Macan, 1954). Boatmen occupy the bottom of the pool, collecting detritus and algal filaments with the anterior legs (Figure 1) (Sutton, 1951). This set of legs have a flattened, scoop shape and are lined with short bristles which act as a shovel to gather particles into the boatman's mouth (Savage, 1990). The most prominent and longest pair of legs are the hind legs, whose metatarsi are covered in hair-like bristles called setae, that when spread give the boatman its recognizable paddle-like appendages (Figure 2) (Peters & Spurgeon, 1971). The middle pair of legs are longer than the anterior pair and adorned with bristle-like structures that aid in standing on the bottom of the pool (Hungerford, 1919). Boatmen carry a temporary air store containing oxygen under their wings while submerged, increasing buoyancy, thus using the bristles of their middle legs to grasp onto rocks and plants to avoid floating to the surface (Parsons, 1976). This gas bubble, held onto setae on the abdomen, allows the boatman to breathe while submerged by filling pores connected to the tracheal system with oxygen (Buck, 1962). The boatman is able to stay submerged, breathing from this air store until the bubble shrinks below a critical size, causing the boatman to swim to the surface to recollect oxygen (Popham, 1960).

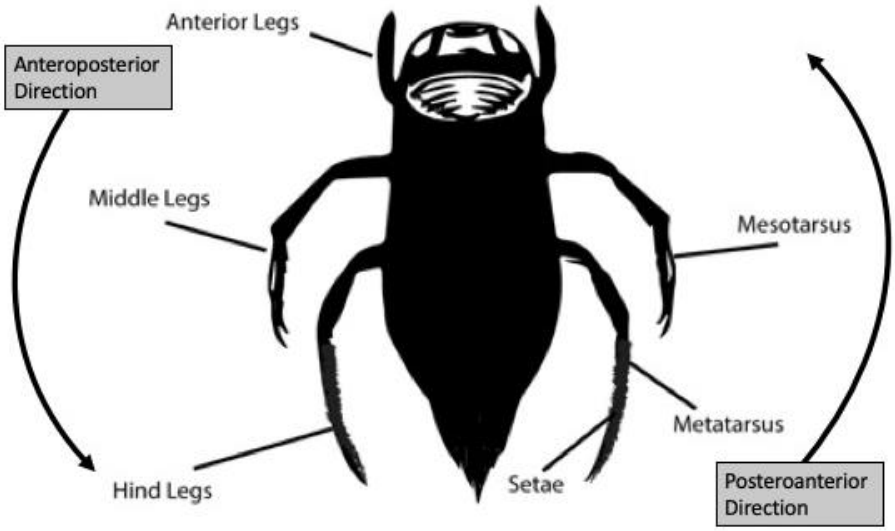

Figure 1. Schematic of Water Boatman Legs indicating direction of motion exhibited by hind legs during rowing

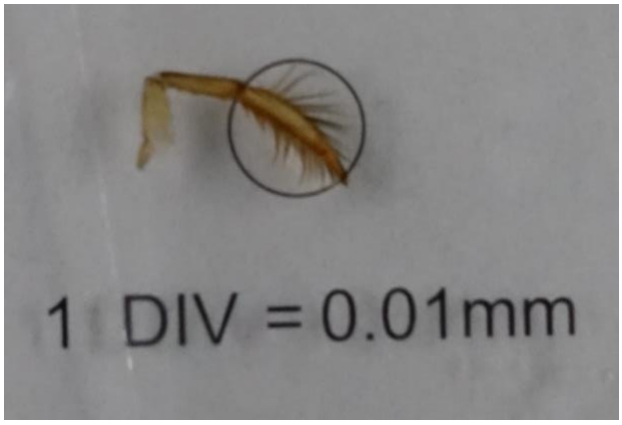

Figure 2. Water Boatman Paddle Splayed (photo taken with Sony RX100-IV)

The boatman's hind paddles operate as a rowing mechanism, creating the thrust needed to move through the water. As the boatman swims, its hind legs rotate anteroposteriorly at a high angle of attack during the power stroke (Ngo & McHenry, 2014). During this stroke, the hindlimbs fully extend, with the setae splayed perpendicularly to the direction of the motion

(Figure 3), while the middle legs have not been observed to play as significant a role in generating thrust to propel the animal forward (Blake, 1986). The reverse motion occurs during the recovery stroke as the hind legs rotate posteroanteriorly to realign with the long axis of the body, and the setae collapse against the metatarsus (Blake, 1986).

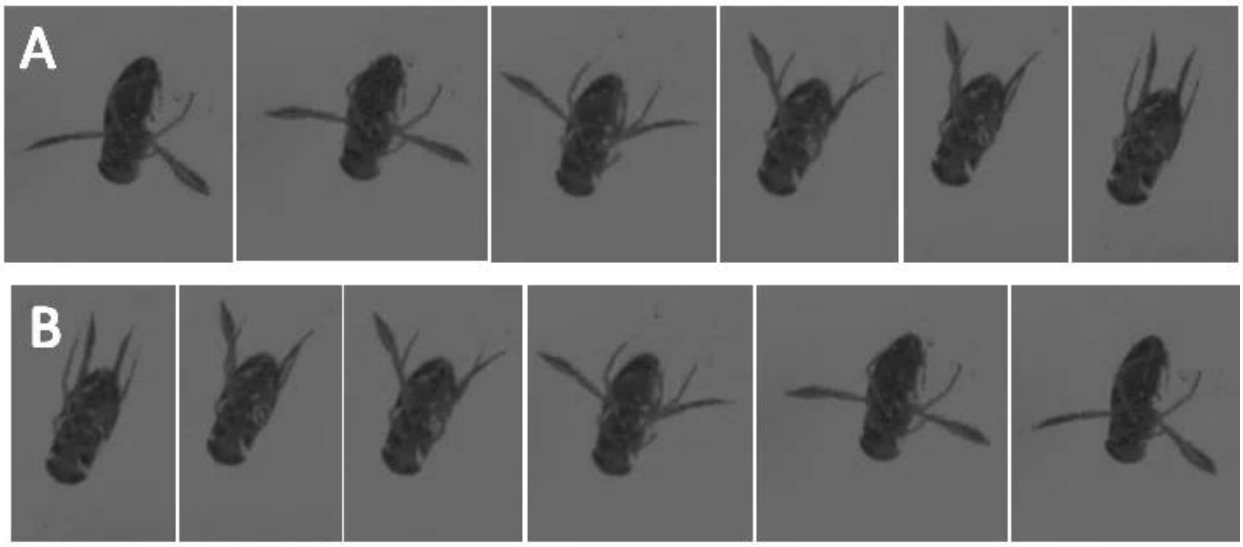

Figure 3. Power Stroke (A) versus Recovery Stroke (B) (video footage of 10 frames taken with Chronos 1.4, Kron Technologies Inc.)

The next section outlines past studies analyzing water boatmen locomotion and the principal fluid forces contributing to the propulsion mechanisms of the overall metatarsus motion. In the following sections, we detail the experimental methods and results attempting to analyze the effect of these fluid forces. These methods include exploring the effects of the changing area of the open paddle compared to the closed paddle using high speed cinematography. We also explore the biological implications of the water boatmen escape

response to stimulus and lay a foundation to understand the physiological details of the boatman's maneuverability using micro-CT scanning.

Chapter 2

Literature Review

Fluid forces that influence aquatic animal swimming at intermediate Reynolds numbers include skin friction, pressure drag, and the acceleration reaction (Vogel, 1996). This acceleration reaction, also called the added mass force, arises as a result of the need for the swimming body to accelerate both its own mass and the mass of the fluid that is dragged alongside the body due to viscous forces (Lighthill, 1971). The "added mass" of the fluid is non-negligible at low Re, creating the need for additional force to accelerate both the mass of the body and the fluid dragged with it (Wainwright & Day, 2007). This acceleration reaction takes into account the unsteady nature of locomotion in aquatic animals: the changing velocity in oscillating appendages and the nonnegligible density of the fluid surrounding these appendages means that this force cannot be neglected (Daniel, 1984). For animals accelerating in a fluid from rest, this force has the potential to generate thrust and has important biological implications for motions such as the escape response (Daniel, 1984). Blake found this acceleration reaction to be a key propulsive force in water boatmen propulsion, while Williams found this force to be much smaller for *Artemia* operating between $1 < Re < 10$, a lower range than that of the boatmen (Blake, 1986), (Williams, 1994). Ngo and McHenry's study on water boatmen at intermediate Reynolds number ($10 < Re < 200$) also failed to find a conclusive major role of the acceleration reaction in thrust generation (Ngo & McHenry, 2014). For the aquatic worm *Sagitta elegans*

operating at a Reynolds number higher than that of the boatman (Re ~ 1000), Jordan found the acceleration reaction did play a role in propulsion (Jordan, 1992). Similarly, in a study of swimming eels, operating at size scales and Re much larger than those of the water boatman (Re ~ 60000), Tytell and Lauder found the acceleration reaction did play a role in propulsion (Tytell & Lauder, 2004), indicating this force should be considered as Re approaches 1000 (Ngo & McHenry, 2014).

While identifying the fluid forces acting on the entire appendage is critical to understanding propulsion, morphology and physiology also play an important role in the locomotion of the animal (Dickinson et al., 2000). In many aquatic insects, setae have important physiological functions which can be examined in more detail. Setae of aquatic insects are hair-like bristles protruding from the body and limbs which can have a variety of functions including locomotion, defense, camouflage, and prey capture (Winterton, 2009). In the water boatman, the setae protruding from the metatarsi serve a locomotory function, expanding into a paddle-like appendage during the power stroke (Ngo & McHenry, 2014). As the paddle of the boatman sweeps through the water, a volume of fluid will pass through the space between the setae. The ratio of this volume of fluid flowing between each setae to the total volume swept by the appendage is defined as its "leakiness" (Figure 4) (Cheer & Koehl, 1987b). Leakiness is used to determine how well the setal appendage is able to produce thrust as fluid moves both around and through the paddle (Koehl, 1995). Rather than considering the Reynolds number of the entire paddle as Blake and Ngo/McHenry did, we can analyze the Reynolds number of individual setae. Setae with a very low Re, where viscosity is more influential than inertia, will have a thicker shear gradient, indicating that some fluid will stick to the setae rather than passing through the spaces between them (Cheer & Koehl, 1987a). Setae with a higher Re will have a less severe

shear gradient, allowing more fluid to pass through the array of hairs. Looking at the Re of the setae in comparison to the Re of the entire appendage allows us to consider how thrust generation may be affected by fluid leaking through the metatarsal during propulsion.

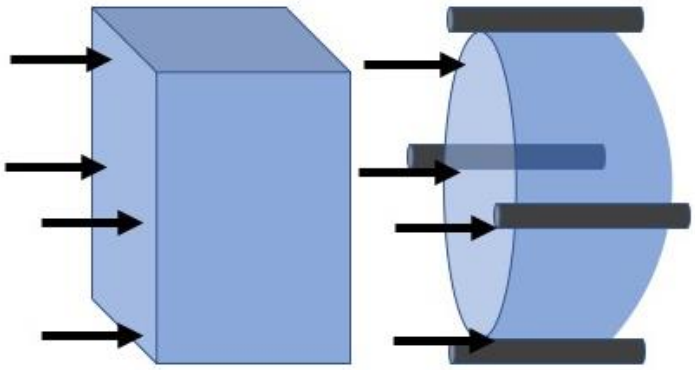

Figure 4. Leakiness is defined as the ratio of the volume of fluid flowing between seta modeled as cylinders (left) to the total volume swept by the setal appendage (right)

Cheer and Koehl found that setae for a variety of animals operate at Reynolds numbers on the order of $10^{-6} < Re_s < 1$ (Cheer & Koehl, 1987b). For $Re_s < 10^{-3}$, setal appendages act as nearly-solid paddles; little fluid is able to leak in between each pair of setae (Koehl, 1996). Comparatively, setal appendages at higher Re ($Re_s > 10^{-2}$) experience greater leakiness, as more fluid is able to move between hairs (Koehl, 1996). These appendages act as sieves and often operate as a mechanism for respiration or feeding (Cheer & Koehl, 1987b). Differentiating whether an appendage operates with a higher or lower leakiness aids in understanding the intensity of the shear gradient around setae and the functionality of the appendage. This functionality has important biological implications for the uses of these appendages. A higher leakiness would allow an appendage to act as a sieve for feeding, as a greater volume of fluid containing food particles may pass through the array of setae (Cheer & Koehl, 1987a).

Conversely, an appendage with a lower leakiness may act as a paddle for grasping food particles (Koehl & Strickier, 1981). Leakiness can also be used to analyze propulsion strategies as paddle-like appendages are intended to be used for locomotion, whereas a sieve-like appendage may be used for respiration (Cheer & Koehl, 1987b).

Morphology can also play a part in the Re of the paddle, affecting the leakiness parameter by varying velocities and distances between setae (Cheer & Koehl, 1987b). As the paddle travels in an arc during propulsion, the tip of the setae travel faster than the basal end, causing the tip to sweep over a higher volume of water (Cheer & Koehl, 1987b). This fact, in addition to the typical nature of setae to be further apart at the distal end compared to at the base, would result in a varying leakiness along the appendage (Koehl, 2004). In the case of the water boatman, as the paddle rows through the power stroke, the surface area of fluid swept by the appendage increases as the setae expand. This increase in area during the power stroke (and decrease during the recovery stroke) changes the morphology of the limb through the propulsion cycle. The effects of this area change have not been heavily studied in the literature, leaving room for our pursuit on this topic.

While the fluid forces of intermediate Re swimming have been studied for a variety of animals, there have been few studies on these forces' impact on water boatmen locomotion specifically. To observe the forces acting on the water boatman as it swims in varying Re regions, Ngo and McHenry tethered boatmen of varying sizes and measured the deflections of the tether as the animal swam, indirectly measuring the thrust generated from swimming (Ngo & McHenry, 2014). Analyzing boatmen of varying lengths (5.0-8.8 mm), specimens were tethered to a fixed point and deflections of the tether were imaged to determine the thrust force generated by swimming. These data were used to track the velocities and positions experienced by the

hindlimbs during the power and recovery strokes, finding paddle Re to vary from $31 < Re < 130$. Ngo and McHenry used high speed video data to show that peak thrust (due to both skin friction and pressure drag) occurred at the peak speeds of the power stroke. Because this motion fell into the intermediate Re regime, the experimenters were interested in the relative roles of pressure vs. skin friction drag. Ngo and McHenry developed a model of both pressure drag and skin friction, finding that only the pressure drag model was able to predict rapid changes in thrust shown by the kinematic data of the tethered boatman experiment, thus suggesting pressure drag is the leading contributor to thrust generation.

While a tethered boatman allows for an adequate analysis of the kinematics describing the propulsive forces, some authors have explored more natural locomotion using high speed cinematography of free swimming (Ngo & McHenry, 2014), (Blake, 1986). Ngo and McHenry found that for free swimming boatmen having body lengths between 2.7-7.7 mm and operating between $3 < Re < 70$, the paddles of the hindlimbs were the leading contributor to forward propulsion (Ngo & McHenry, 2014). Similar results were achieved by Blake, who also found that for free swimming boatmen (8.5 mm in length) analyzed under high speed cinematography, the hind legs were the only appendages involved in generating thrust needed to overcome the drag felt by the body (Blake, 1986). Due to the unsteady nature of rowing and the assumption that the boatman does not move at a constant velocity, Blake also took the acceleration reaction force into consideration as a contributor to thrust generation (Blake, 1986). Ngo and McHenry, however, found that for free swimming at intermediate Re, this acceleration reaction played only a minor role in propulsion (Ngo & McHenry, 2014).

The three forces that have the potential to play a role in water boatmen locomotion at intermediate Reynolds number include skin friction, pressure drag, and the acceleration reaction.

These forces are dependent on both the flow around the entire metatarsus, as well as the leakiness through the array of setae making up the metatarsal paddle. While previous studies on water boatman locomotion focused on drag force analysis, the change in area the paddle experiences during the power stroke has yet to be studied. This study aims to analyze how the combination of these forces generates the thrust needed to propel water boatmen through the intermediate Reynolds number regime. This study also explores the implications of the change in area of the paddle as the setae are splayed through the power stroke, as observed using high speed cinematography.

Chapter 3

Methods

Collection of Animals

Animals for this study were collected on a periodic basis from Ten Acre Pond (Pennsylvania State Game Lands No. 176) or Millbrook Marsh, both in State College, Pennsylvania (Figure 4). We found water boatmen predominately along the edges and bottom of the pond using hand nets and buckets. Collections ran on an as-needed basis from August of 2018 to March of 2019 in water temperatures ranging from approximately 4°C to 22°C. We kept specimens in laboratory tanks at room temperature, in a pond and tap water mixture, degassing the tap water to remove chlorine traces before adding boatmen to the tank. Sediment and debris from the collection site were also kept in the tanks to provide a natural environment and detritus for the boatmen to feed on. Boatmen were not fed any additional sustenance and were kept undisturbed until used in experiments with the exception of pumps used to oxygenate the water. We kept boatmen in their laboratory tanks for varying lengths of time ranging from one week to up to three months.

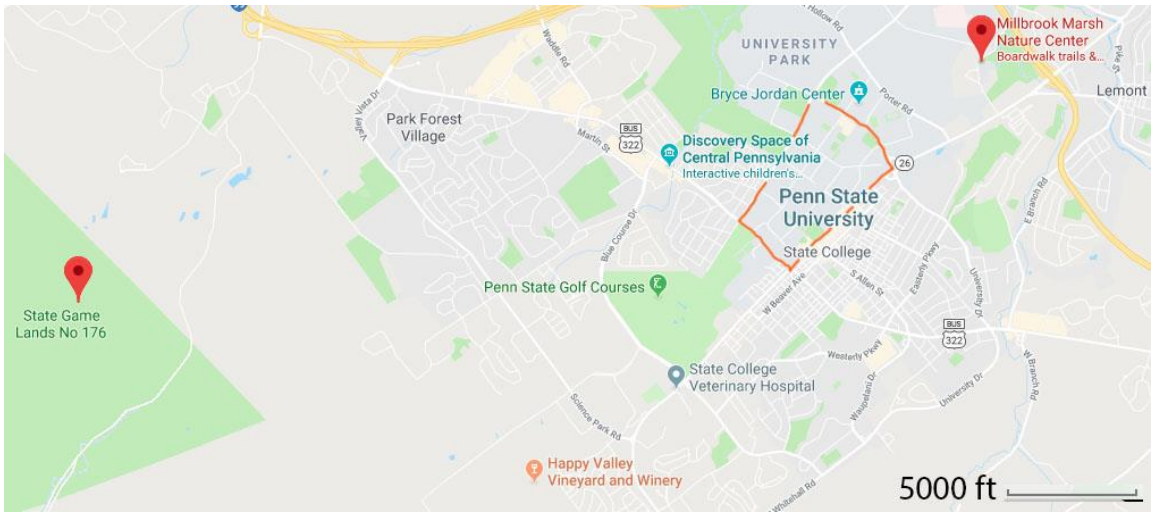

Figure 5. Map of Ten Acre Pond (State Game Land No. 176) and Millbrook Marsh in proximity to Penn State University Campus (orange)

Impulse Chamber Design

To observe the boatman's escape response, we designed and constructed an impulse chamber to provide a repeatable jet impulse for startling a resting boatman. This chamber was designed to trigger the boatman's escape response to stimuli and capture this motion using high speed cinematography. We constructed a 10 x 12 x 6-inch tank out of 0.125-inch clear acrylic panels (Figure 4). Panels were adhered using a combination of SCIGRIP-16 and SCIGRIP-4 fast set acrylic cement. The tank was split into two halves (a test section and an activation section) separated by a solid white acrylic panel, housing a 3D printed sliding track designed using SolidWorks. This sliding track contained a 10 mL syringe to provide a repeatable jet impulse whose horizontal position could be adjusted in alignment with the boatman's position. The test section was lightly layered with pebbles and debris from the boatman's laboratory tank and covered with a clear, removable acrylic lid. The activation section was left open to provide a space to operate the jet without startling the boatman with a visual stimulus. We attached a layer

of foam with a backing adhesive and placed it in the center of tank to encourage boatmen to sit in front of the syringe nozzle. This nozzle could be moved horizontally along the sliding track to ensure that the stimulus was in line with the resting animal. We operated the jet at varying flow rates ranging from 3.5 mL/s to 7 mL/s. Despite repeated trials, boatmen were not predictably responsive to the jet stimulus, leading to the use of a secondary tank for high speed cinematography analysis of kinematics.

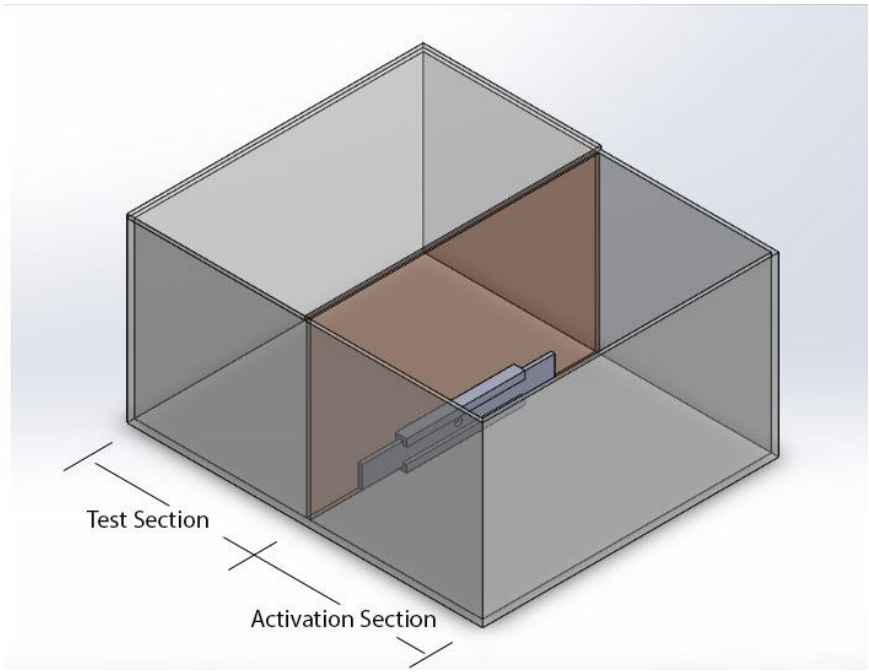

Figure 6. Impulse Chamber Designed for Capturing Boatman Escape Response

High Speed Cinematography

To perform high speed cinematography, we constructed a 4 x 4 x 4-inch tank out of 0.25-inch acrylic panels, adhered using SCIGRIP-16 fast set acrylic cement, and reinforced with silicone. The top of the tank was left open to insert and remove boatman for testing. We placed a paper towel at the bottom of the tank to provide a frictional surface for the boatman to grab.

We also placed pebbles from Ten Acre Pond in the corners of the tank to hold down the paper towel and encourage natural response from boatmen.

Two high speed cameras (Chronos 1.4, Kron Technologies Inc, Burnaby, BC, Canada), were used to collect kinematic data of the boatman's motion. Camera 1 was mounted 18 inches from the front face of the testing tank. Camera 2 was also mounted 18 inches from the testing tank, positioned 90 degrees from Camera 1 (Figure 6). Both cameras recorded at the same frame rate, connected by a manual BNC trigger stop. The testing environment was backlit by two diffuse LED panels, one positioned behind Camera 1 and the other 90 degrees from Camera 1. The simultaneous video streams were calibrated using a 1 x 1-inch calibration plate with 0.5 mm spacing. The calibration plate was mounted at a 45 degree angle from both Camera 1 and Camera 2 inside the testing tank under the surface of the water. Using a microtranslator, the calibration plate was swept over a one-inch distance; three plate locations, at z = -0.5", z = 0", and z = 0.5", were recorded in both cameras. Images from calibration were digitized using the MATLAB DLTdv tool (Hedrick, 2008) to map the pixels into three-dimensional real space using the Direct Linear Transform (Abdel-Aziz, Karara, & Hauck, 2015).

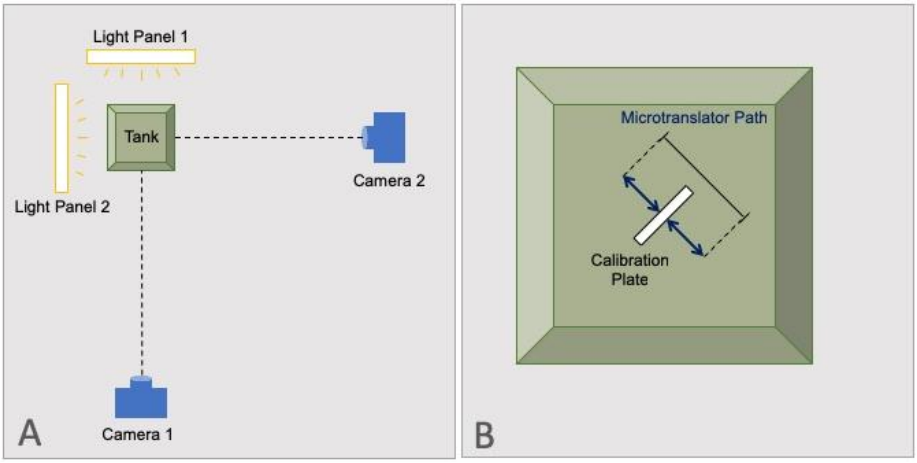

Figure 7. Top view of overall high-speed cinematography setup (A). Top view of tank only indicating direction of motion of the calibration plate using the microtranslator

To capture kinematic data, we moved one boatman from the laboratory tank to the testing tank containing 23°C dechlorinated tap water. Boatmen were given ten minutes to acclimate to the new environment before capturing any footage. After acclimation, both cameras began recording into a ring buffer until the test animal swam to either reposition or breathe at the tank's surface. Using the manual trigger, both cameras were stopped simultaneously and the ring buffer for each camera was stored. This process was repeated for 5 trials on the first boatman, 7 on the next, and 17 on a third boatman on three separate occasions. Boatmen were returned to the laboratory tank after testing. All boatman used in testing were adults.

Microscope Measurements

To determine the parameters needed to analyze leakiness, measurements were taken of the lengths and areas of the open and closed paddles, along with the setal diameter and spacing, using an Olympus BX60 microscope. Boatmen were anesthetized and killed using a mixture of 74% 190-proof ethanol and 26% water. The metatarsi were dissected from the body and placed in water overnight. Measurements were first collected of the paddle in its closed position. Using 10X magnification, the metatarsus was observed under the microscope in water alongside a calibration slide. Images were captured using a DSLR camera (Nikon, D5600). Next, measurements were taken of the fully open paddle. Using insect pins, setae of the metatarsus were spread into their naturally splayed position observed during the power stroke. Microscope images were captured under 5X, 10X, and 40X magnification. Unlike the closed paddle, images of the open paddle were also captured using a Sony RX100-IV camera mounted above the sample, with its optical axis perpendicular to the splayed paddle. Using Fiji-ImageJ (Schneider,

Rasband, & Eliceiri, 2012) measurements were taken of the paddle length (L), major length (l_1), metatarsus width (l_2), minor length (l_3), setae diameter (d), intersetal space (D), area (A), and angle (θ) (Figure 8). ImageJ measurements were taken in comparison to a 1 mm microscope calibration slide and recorded in Table 1.

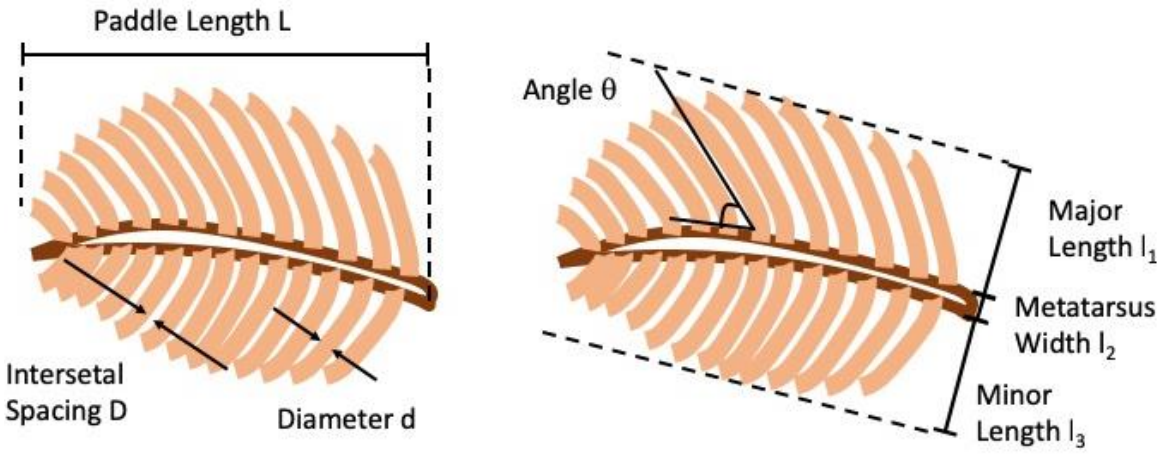

Figure 8. Morphological Paddle Diagram

Table 1. Microscope Paddle Measurements from ImageJ

	Closed Paddle	Open Paddle
Length (L) [mm]	4.55	4.67
Major Length (l_1) [mm]	0.43	0.94
Width (l_2) [mm]	0.50	0.54
Minor Length (l_3) [mm]	0.09	0.93
Diameter (d) [mm]	0.005	0.005
Intersetal Spacing (D) [mm]	0.04	0.004
Area (A) [mm^2]	4.13	9.69
Angle (θ) [deg]	24.0	64.3

Micro-CT Scanning

Micro-CT scans of the hind appendages of the boatmen were used to provide a detailed look at the joint structure to better understand how boatman physiology plays a role in the mechanics of swimming. These scans were performed by the Energy and Environmental Sustainability Laboratory at the Pennsylvania State University using the GE v|tome|x L300 multi-scale micro-CT system. High resolution scans were used to analyze morphological details of the muscle structures and tissues that contribute to motion of the hind legs. To perform scans at a high resolution, we stained test specimens using an iodine-ethanol solution. Three animals were euthanized in a 70% ethanol solution and placed in tincture of iodine to stain for 94 hours. We completely submerged all samples in the stain, stirring periodically to ensure the iodine penetrated the tissues. We then washed the samples in 190-proof ethanol for one to three hours immediately before scanning. Once prepared, animals were staged in a fast-solidifying wax inside a pipette tube to ensure samples did not move during scanning. Two scans of the entire animal were performed at 10 um resolutions, the hindlimbs were scanned at 2 um and 3 um resolution. These micro-CT scans were intended to show the boatman's musculoskeletal system for a better understanding on the rotational and translational motions each joint is able to experience.

Chapter 4

Results

Biological Implications

High speed cinematography of boatman swimming motion in both the impulse chamber and the smaller testing tanks revealed several of the boatman's biological tendencies. Despite repeated trials at varying flow rates, the boatman was unresponsive to the jet stimulus of the impulse chamber. This lack of a response could be an indication of a slow escape response time, or may be a product of lethargic boatmen, as animals were not fed during captivity. The small testing tank revealed three categories of behavior: grooming, breathing, and repositioning. Of the 25 high speed videos which clearly demonstrated one of these characteristic behaviors, four displayed grooming, three displayed breathing at the surface, and 18 displayed repositioning without surfacing. This repeated behavior of the boatman moving from rest to a new position in the tank without surfacing may be indicative of food seeking. Boatmen were not externally disturbed during these trials, suggesting that repositioning behavior may be part of a survival instinct to search for a food source once in a new location. The boatmen displayed this behavior every several minutes, in addition to their breathing and grooming behaviors which occurred far less frequently.

The lack of response to the jet stimulus of the impulse chamber also leaves room for future work on the water boatman escape response. Failure to gain a repeatable and predictable

response from the maximum jet impulse indicates that boatmen are not perturbed by jet flows lower than 7 mL/s. Future work should use higher flow rates, or use jets more directly positioned toward the resting boatman. The lack of response to the jet may also indicate that a water jet does not correspond to a naturally-occurring threat, and that boatmen may be more likely to be stimulated by a physical response indicative of a threat. Threatening physical stimuli could include prodding a resting boatman with an object rather than a flow stream. The survival instinct may also be triggered by introducing the scent of predators that feed on boatmen to an environment originally free of any threats. These additional stimuli would potentially activate the animal's survival instinct and provoke the desired response.

Area Measurements and Implications of Maneuverability of Hairy Appendages

After recording synchronized high speed footage from the 4 x 4-inch testing tank, we converted videos from both cameras to their individual frames from an mp4 format to a TIFF image sequence using Adobe Photoshop (Adobe Inc., San Jose, CA). These image sequences were manually examined frame-by-frame to identify 1) frames displaying the boatman paddle in a fully open position and 2) a fully closed position, in which the paddle was visible from both camera views. Image sequences of the paddle expanding to the fully open position (power stroke) and collapsing into the fully closed position (recovery stroke) were identified and converted into an AVI format for video analysis of footage containing just one swimming cycle. To collect area measurements of the area swept by the paddle, we used Fiji-ImageJ (Schneider et al., 2012) to select the area of the paddle at the moment that the boatman's metatarsus splayed parallel to the camera. Using the built-in Fiji-ImageJ measurement tool, we measured paddle

area of the fully closed position as well as the fully open position (Figure 9). Using video footage containing 60-100 frames per test, we measured the paddle area (in number of pixels) every three to five frames. We plotted the absolute (non-normalized) area data (A) in pixels versus the frame number (N) for several video trials to approximate the total area swept by the paddle through one power and one recovery stroke (Figure 10).

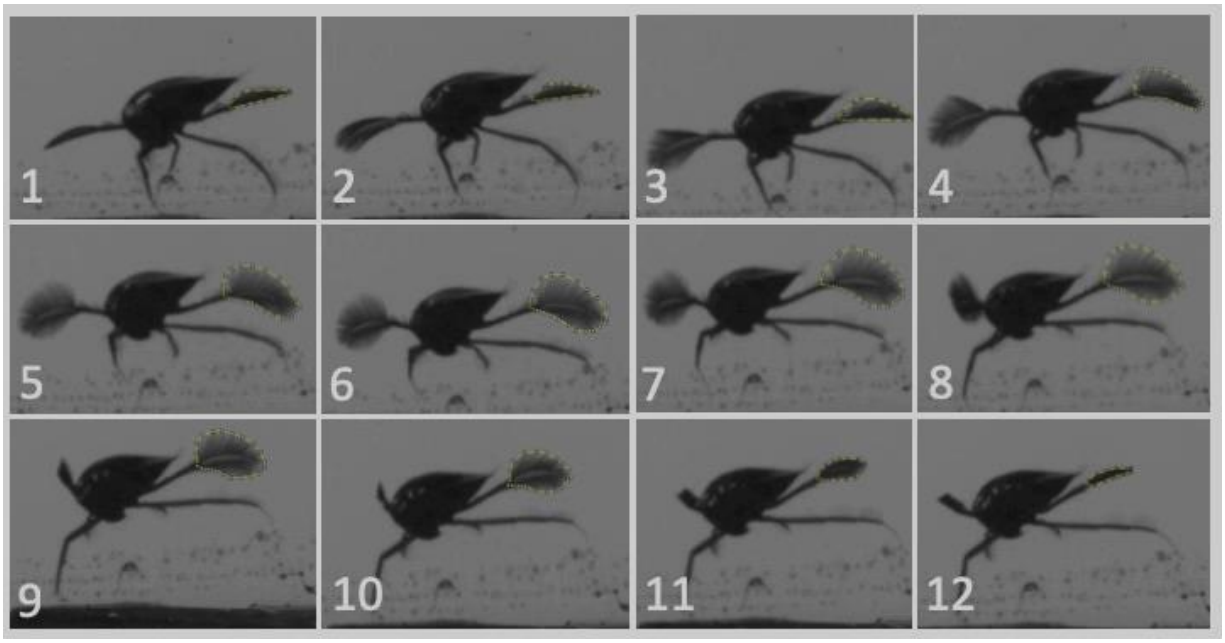

Figure 9. ImageJ selections of paddle area (yellow) through one power stroke and one recovery stroke

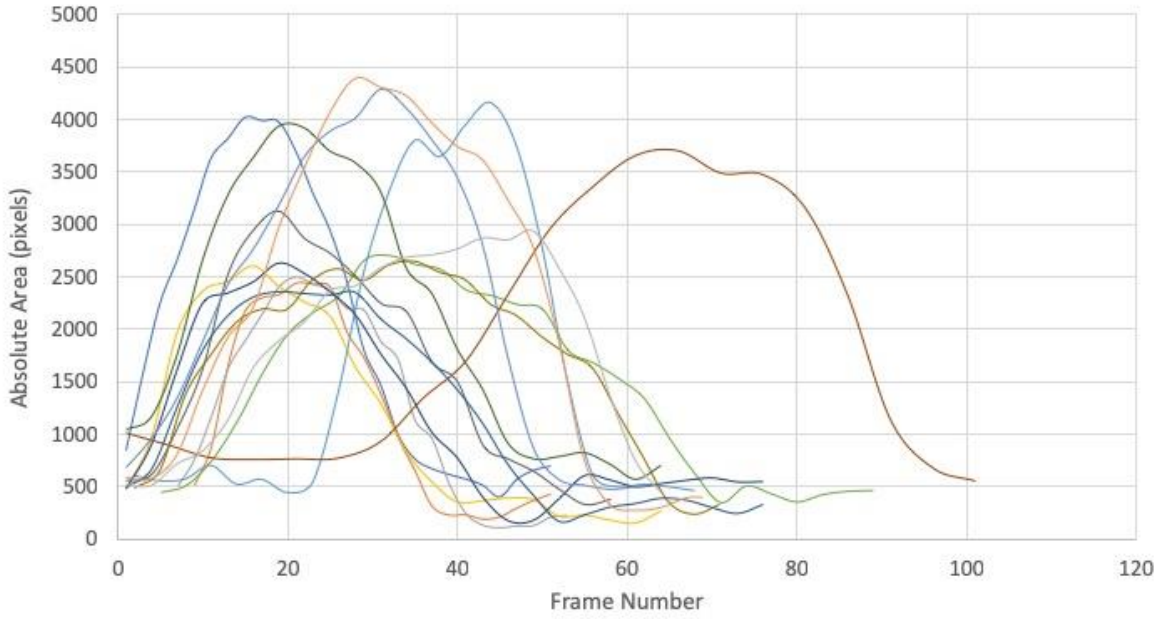

Figure 10. Absolute Area vs. Frame Number data obtained from Fiji-ImageJ of setae splayed through power and recovery stroke

Raw area measurements were normalized by converting the frame number used by ImageJ into real-time as originally recorded by the camera. Every video recorded 17,472 frames at a rate of 1057.362 frames per second. From this frame rate, the amount of time between two consecutive frames was 0.95 ms. Conversions from the original mp4 format to the TIFF sequence saved every frame, indicating that the time step between consecutive frames remained 0.95 ms. Similarly, conversions from the TIFF sequence into an AVI format also imported every frame, indicating that the final data points plotted in Figure 10 maintained a time step of 0.95 ms between two consecutive frames. We then normalized the area measurements, originally recorded by ImageJ in number of pixels, to a non-dimensional area by taking the ratio of area pixels to the minimum area recorded for each video (Figure 11). This normalized plot demonstrated the percent change in area throughout one swimming cycle. Likewise, we normalized the area measurements using the ratio of area pixels to the maximum area recorded

for each video (Figure 12). This method of normalizing the data allowed us to see the ratio of the area swept by the paddle and the time needed to complete one power and one recovery stroke.

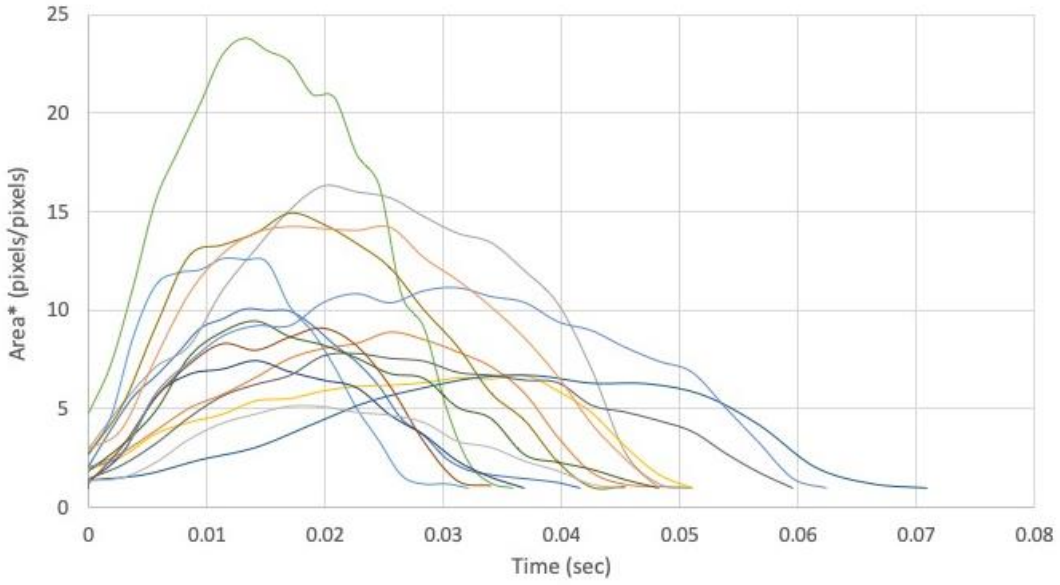

Figure 11. Normalized Area by Minimum vs. Time obtained by non-dimensionalizing data obtained from ImageJ

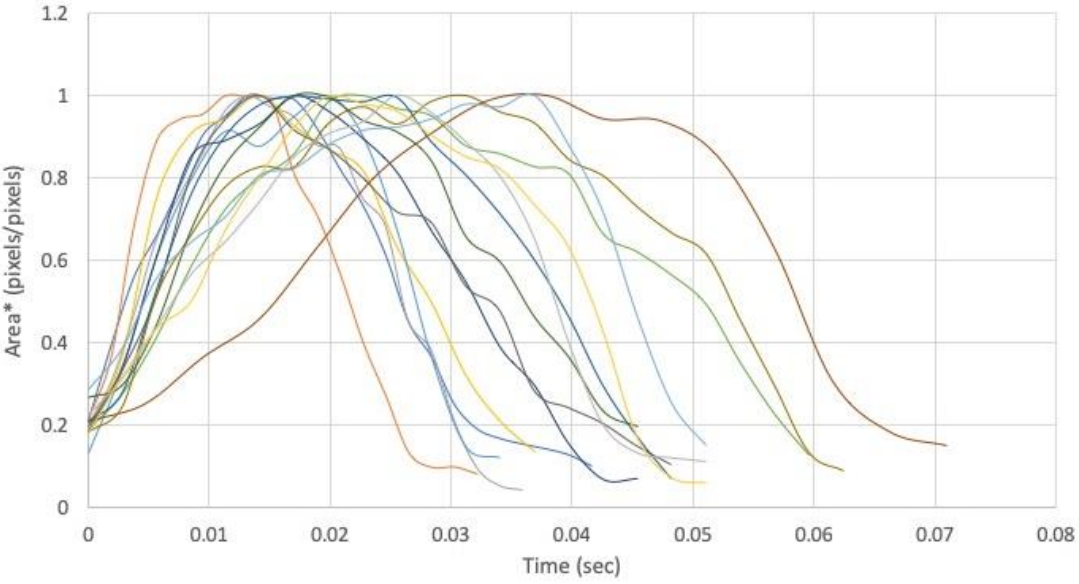

Figure 12. Normalized Area by Maximum vs. Time obtained by non-dimensionalizing data obtained from ImageJ

Figure 11, shows the percent increase in area (A/A_{min}) as a function of time. The maximum percent change can be seen where the boatman has expanded the paddle to its fullest extent. This maximum percent change in area ranged from $506\% < A_{\%} < 2380\%$ indicating that boatmen are able to use the setae to dramatically increase the surface area of the metatarsal region during the power stroke. The swimming cycle displaying the largest percent change also occurred in 34 ms, while that of the smallest percent change occurred approximately 1.3 times slower, indicating a potential relationship between velocity and area change. Figure 11 shows this general trend of smaller changes in percent area to occur for longer swimming cycles, while much greater changes in percent area occur more rapidly. This pattern suggests one of two conclusions: 1) that boatman must splay a much greater area of setae to move through one swimming cycle in a shorter amount of time, or 2) the setal splaying is passive, and a higher velocity during the power stroke forces the setae to splay more. This may be indicative of a survival characteristic suggesting that boatman able to extend their setae to larger paddles may be able to maneuver through the water faster.

Normalizing the paddle area by the maximum (Figure 12) demonstrates that the time needed to complete one swimming cycle varied among strokes. The time to complete one swimming cycle ranged from $32 \text{ ms} < t < 71 \text{ ms}$. If the boatmen had not been varying the speed at which paddle area increases, the plots of normalized area for each trial (Figure 12) would have collapsed into one curve, indicating that the paddle splays at the same rate for every stroke. However, the range of times shown indicates a boatman's ability to (passively or actively) vary the paddle expansion speed through the power and recovery strokes. The variability in time taken for one swimming cycle suggests the boatman is able to control both the frequency of the power and recovery stroke and the speed at which setae expand. This suggests the

maneuverability of setal appendages is important to locomotion in the water boatman. Expanding/collapsing the setae of the paddle (and thus increasing/decreasing the paddle area at varying rates) allows the boatman to manipulate its appendages appropriately to achieve different motions such as propulsion and turning.

Using the time steps plotted in Figures 10-12, we were able to measure the length of time of one swimming cycle for each trial. By looking at the slope (dA/dN) of the raw measurements (Figure 10), we determined the power stroke to begin when dA/dN was greater than 100 pixels/number of frames. We determined the recovery stroke to end when dA/dN was a minimum, as this point indicated that following frames were the beginning of the next power stroke. This method of identifying the length of time of one swimming cycle points out some of the limitations of 2D video analysis. For example, in some trials the boatman's paddle may not have been completely parallel to the camera's view due to its manipulation of the wrist joint while propelling. This alters the area measurement taken from ImageJ at points where the paddle is actually at an angle, measuring a projected area less than the actual area. However, this error accounted for only a small percentage of test measurements, allowing us to observe an overall pattern in the time step and area measurement of the boatman's swimming cycle.

Implications of Re and Leakiness Parameters

Using the length of time per one swimming cycle obtained from Figures 10-12, we found the Re_s of the paddle's setae for each trial. We measured the angular velocity of the limb using the time recorded to move through one swimming cycle (Δt) and the angle (α) swept by the hindlimb of the boatman. This velocity calculation assumes the tip of setae move at the same

speed as the tip of the hindlimb; since the setae cluster around the distal end of the hindlimb, this approximation is appropriate. The angle traveled by the hindlimb was approximated to range from 45 deg < α < 165 deg (Ngo & McHenry, 2014). The angular velocity (ω) is given by:

$$\omega = \frac{\alpha}{\Delta t}$$

The tangential velocity (u) of the hindlimb distal end is therefore given by:

$$u = \omega * L$$

To calculate this tangential velocity we measured (using ImageJ) the length of the boatman's entire hindlimb (L) on frames displaying this limb fully extended. These measurements were calibrated using the 1 x 1-inch calibration plate, determining the length of the limb in mm. To determine the range of Re at which the setae were operating, we used the diameter of the setae as measured in Table 1 and the kinematic viscosity (ν) of water at 23°C. The Re is given by:

$$Re = \frac{u * d}{\nu}$$

We found the Re of the setae to range from $7.1 \times 10^{-1} < Re_s < 2.6$, falling into the low range of intermediate Re. Ngo and McHenry found the Re of the entire paddle to operate between $3 < Re_p < 70$ (Ngo & McHenry, 2014), indicating that viscous forces are more dominant around the setae than around the metatarsal itself by one order of magnitude.

We also calculated the "leakiness" of the hindlimb, as defined by Cheer and Koehl, to determine if these appendages behave as paddles or rakes/sieves (Cheer & Koehl, 1987b). For Re < 1 leakiness is defined by the intersetal spacing (D), setae diameter (d), and paddle length (L) and is given by:

$$Leakiness = \frac{D^3}{d * L^2}$$

Using morphological data from Table 1, leakiness of the boatman's paddle falls on the order of 10^{-7}. Such a low leakiness value indicates these appendages function as paddles. As Re values approach 1, these appendages will have higher leakiness values, operating like leaky paddles (Cheer & Koehl, 1987b). Because leakiness depends on the morphology of the appendage in addition to its Re, both the size and speed of the boatman will have an impact on the leakiness. Our findings indicate that boatman setae operate in the Re_s range ($10^{-2} < Re_s < 1$) at which these changes in size and speed have significant effects on leakiness (Koehl, 1996). This range suggests that leakiness of the boatman's paddle may change significantly as boatmen grow from juveniles to adults. These changes in the leakiness parameter may alter the functionality of the metatarsal between those of a rake and a paddle, impacting locomotion and feeding strategies. The possible differences between leakiness and its impact on functionality of boatmen appendages through various stages of life leaves room for future exploration of this topic.

Micro-CT Analysis

High resolution micro-CT scans of the water boatman's body and hind limbs provided x-ray images of boatman physiological details. X-ray images of slices through the body were reconstructed into 3D images detailing muscle structures, internal organs, and insect tissues that make up a majority of the boatman's musculoskeletal system. The scans were intended to show the individual leg joints and the joints connecting the hindlimbs to the body to gain a deeper understanding of the nature of the motions experienced by each part of the limb. Images of these joints were also intended to show if boatmen rely on hinge joints or ball-in-socket joints to move appendages during propulsion. Our scans displayed five joints of the boatman's hindlimbs and

the muscular segments making up the anterior legs (Figures 13), although we could not identify the joint types of each segment due to insufficient resolution.

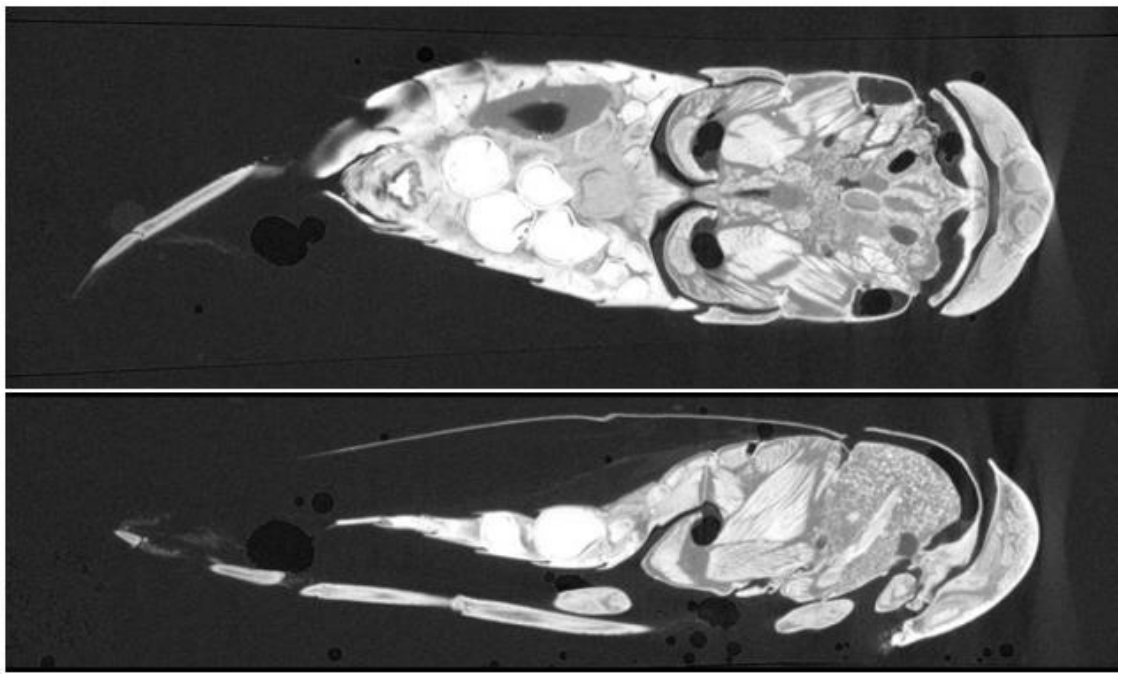

Figure 13. Micro-CT scan of boatman body at 10 um top view (top) and side view (bottom)

Use of micro-CT scans on the boatman's appendages could be used in future studies to gain knowledge of the hindlimb mechanism used in propulsion. Views of the joints would be used for a better understanding of the rotation and translation each part of the limb can experience, leading to potential use in computational models of the mechanics of swimming at intermediate Re. Knowledge of the nature of the limbs and their mechanics would provide another avenue for understanding thrust at intermediate Re, in addition to kinematic and hydrodynamic studies. Future work using high resolution micro-CT scans could also provide information on propulsion at the small scales at which the boatman operates, opening new biological questions on these propulsion strategies.

Chapter 5

Conclusions

The aim of this study was to gain a deeper understanding of the interactions between a water boatman's hind appendage and the fluid it swims through. These interactions are not well understood for the intermediate Reynolds numbers at which the boatman operates, as both inertial and viscous forces may contribute to the drag generated by the boatman. This study used high-speed cinematography to capture both stimulated and natural locomotion of the animal, focusing on the morphology and motion of the hairy appendages. Analysis of the changing area of the paddle as setae splay during the power stroke and collapse during the recovery stroke, combined with the calculated leakiness parameter, suggest a boatman's metatarsi do act as paddles during propulsion.

Video data displaying the change in area of the paddle demonstrated both an ability to control the speed of splaying setae and a trend between percent area increase and time to complete one swimming cycle. The observed trends indicate the boatman's tendency to expand the paddle much larger at a much faster rate. The ability to control paddle speed suggests that maneuverability is a key component of water boatmen locomotion, as splaying the setae at different rates may be used to achieve faster propulsion or turns of the body. Alternatively, the setal splaying may be a passive response to faster motion through the water; future work will focus on understanding the passive vs. active nature of the setal splaying. In either case, this change in area of hairy appendages leaves room for future work on the biological implications of expanding setae at a faster or slower rate.

Calculations of the Re_s of the setae suggest that the metatarsi operate on the low end of the intermediate Re regime, indicating that inertial and viscous forces are at play over both the entire paddle, as observed by Blake and Ngo/McHenry, and over the setae themselves. The low leakiness of these setae indicates that the metatarsi act as paddles, although the intermediate Re regime suggests that differences in size and speed will have significant changes on the leakiness parameter. This may play a role in the functionality of the paddle as the boatman ages from juvenility to adulthood, thus changing the spacing of setae and the speeds at which these setae operate. Further exploration on this difference in leakiness between a juvenile and adult could give way to further insight on the changing functionality of hairy appendages during maturation. Changes in this morphology, combined with a further understanding of the physiology of the boatman's hindlimbs using micro-CT scans, would provide a more complete picture on the mechanics of propulsion at small scales. Understanding the morphology of the paddle and the impact of controlling its speed gives rise to potential future work on the fluid interactions between this animal and the water.

BIBLIOGRAPHY

Abdel-Aziz, Y. ., Karara, H. M., & Hauck, M. (2015). Direct Linear Transformation from Comparator Coordinates into Object Space Coordinates in Close-Range Photogrammetry. *Photogrammetric Engineering & Remote Sensing*, *81*(2), 103–107.

Blake, R. W. (1986). Hydrodynamics of swimming in the water boatman, Cenocorixa bifida. *Canadian Journal of Zoology*, *64*(8), 1606–1613.

Buck, J. (1962). Some Physical Aspects of Insect Respiration. *Annual Review of Entomology*, *7*(1), 27–56.

Cheer, A. Y. L., & Koehl, M. A. R. (1987a). Fluid Flow through Filtering Appendages of Insects. *Mathematical Medicine and Biology: A Journal of the IMA*, *4*(3), 185–199.

Cheer, A. Y. L., & Koehl, M. A. R. (1987b). Paddles and rakes: Fluid flow through bristled appendages of small organisms. *Journal of Theoretical Biology*, *129*(1), 17–39.

Childress, S. (1981). *Mechanics of swimming and flying*. Cambridge University Press.

Daniel, T. L. (1984). Unsteady Aspects of Aquatic Locomotion. *American Zoologist*, *24*(1), 121–134.

Dickinson, M. H., Farley, C. T., Full, R. J., Koehl, M. A., Kram, R., & Lehman, S. (2000). How animals move: an integrative view. *Science (New York, N.Y.)*, *288*(5463), 100–106.

Fish, F. E., & Lauder, G. V. (2006). PASSIVE AND ACTIVE FLOW CONTROL BY SWIMMING FISHES AND MAMMALS. *Annual Review of Fluid Mechanics*, *38*(1), 193–224.

Godoy-Diana, R., & Thiria, B. (2018). On the diverse roles of fluid dynamic drag in animal swimming and flying. *Journal of The Royal Society Interface*, *15*(139), 20170715.

Hedrick, T. L. (2008). Software techniques for two- and three-dimensional kinematic measurements of biological and biomimetic systems. *Bioinspiration & Biomimetics*, *3*(3), 034001.

Hungerford, H. B. (1919). *The Biology and Ecology of Aquatic and Semiaquatic Hemiptera: The Male Genitalia as Characters of Specific Value in Certain Cryptocerata (Hemiptera-Heteroptera)* (Vol. 11). The University.

Jordan, C. E. (1992). A Model of Rapid-Start Swimming At Intermediate Reynolds Number: Undulatory Locomotion in the Chaetognath Sagitta Elegans. *Journal of Experimental Biology*, *163*(1), 119–137.

Koehl, M. A. R. (1995). Fluid Flow through hair-bearing appendages: feeding, smelling and swimming at low and intermediate Reynolds numbers. *Symposia of the Society for Experimental Biology*, *49*, 157–182.

Koehl, M. A. R. (1996). When Does Morphology Matter? *Annual Review Ecology and Systematics*, *27*(1), 501–543.

Koehl, M. A. R. (2004). Biomechanics of microscopic appendages: functional shifts caused by changes in speed. *Journal of Biomechanics*, *37*(6), 789–795.

Koehl, M. A. R., & Strickier, J. R. (1981). Copepod feeding currents: Food capture at low Reynolds number. *Limnology and Oceanography*, *26*(6), 1062–1073.

Lighthill, M. J. (1969). Hydromechanics of aquatic animal propulsion. *Annual Review of Fluid Mechanics*, *1*(1), 413–446.

Lighthill, M. J. (1971). Large-amplitude elongated-body theory of fish locomotion. *Proceedings*

of the Royal Society of London. Series B. Biological Sciences, *179*(1055), 125–138.

Macan, T. T. (1954). A Contribution to the Study of the Ecology of Corixidae (Hemipt.). *The Journal of Animal Ecology*, *23*(1), 115–141.

Ngo, V., & McHenry, M. J. (2014). The hydrodynamics of swimming at intermediate Reynolds numbers in the water boatman (Corixidae). *The Journal of Experimental Biology*, *217*(15), 2740 LP-2751.

Parsons, M. C. (1976). Respiratory Significance of the Thoracic and Abdominal Morphology of Three Corixidae, DiaPrepocoris, Micronecta, and Hesperocorixa (Hemiptera: Heteroptera: Hydrocorisae). *Psyche: A Journal of Entomology*, *83*(2), 132–179.

Peters, W., & Spurgeon, J. (1971). Biology of the Water-boatman Krizousacorixa femorata (Heteroptera: Corixidae). *American Midland Naturalist*, *86*(1), 197–207.

Popham, E. J. (1960). ON THE RESPIRATION OF AQUATIC HEMIPTERA HETEROPTERA WITH SPECIAL REFERENCE TO THE CORIXIDAE. *Proceedings of the Zoological Society of London*, *135*(2), 209–242.

Purcell, E. M. (1977). Life at Low Reynolds number. *American Journal of Physics*, *45*(1), 3–11.

Savage, A. A. (1990). Lesser Water Boatmen (Corixidae). *Field Studies*, *7*, 485–515.

Schneider, C. A., Rasband, W. S., & Eliceiri, K. W. (2012). NIH Image to ImageJ: 25 years of image analysis. *Nature Methods*, *9*(7), 671–675.

Sutton, M. F. (1951). On the food, feeding mechanism and alimentary canal of Corixidae (Hemiptera, Heteroptera). *Proceedings of the Zoological Society of London*, *121*(3), 465–499.

Tytell, E. D., & Lauder, G. V. (2004). The hydrodynamics of eel swimming. *Journal of Experimental Biology*, *203*(20), 3103–3116.

Vogel, S. (1996). *Life in moving fluids: the physical biology of flow*. Princeton University Press.

Wainwright, P. C., & Day, S. W. (2007). The forces exerted by aquatic suction feeders on their prey. *Journal of the Royal Society Interface*, *4*(14), 553–560.

Williams, T. A. (1994). Locomotion in Developing Artemia Larvae: Mechanical Analysis of Antennal Propulsors Based on Large-Scale Physical Models. *The Biological Bulletin*, *187*(2), 156–163.

Winterton, S. L. (2009). Scales and Setae. In *Encyclopedia of Insects* (pp. 901–904). Academic Press.

ACADEMIC VITA

Rebecca Denby

Rjd5394@psu.edu

EDUCATION

Pennsylvania State University, University Park, PA — Graduation: May 2019
Schreyer Honors College
Bachelor of Science in Mechanical Engineering (Honors)

WORK EXPERIENCE

Coherent Technical Services, Lexington Park, MD — May-Aug. 2018
Mechanical Engineering Intern

- Collaborated with team to assist the redesign and simplification of shipboard interrogator system chassis
- Modernized design of shipboard system chassis to support Tactile Panel PC and delivered total drawing package to customer
- Communicated between customers and vendors to locate parts in order to meet project needs
- Reverse engineered shipboard system chassis to obtain drawing package for use in future modifications

United States Census Bureau, Suitland, MD — June-Aug. 2017
Statistical Pathways Intern — June-Aug., Dec. 2016

- Conducted detailed macrodata review and analysis of over 1000 geographic outliers using ArcGIS satellite imagery
- Compiled and presented geographic research findings to senior management to propose changes to annual delivery files for the American Community Survey
- Communicated and trained other employees on the IT requirements conversion process

RESEARCH & PROJECTS

Undergraduate Research, Pennsylvania State University — Jan. 2018-May 2109
Environmental and Biological Fluid Mechanics Lab

- Investigated impact of intermediate Reynolds number on swimming mechanisms of small-scale aquatic insects using 3D Kinematic data
- Wrote undergraduate Schreyer Honors College thesis on intermediate Reynolds number locomotion of the water boatman (*Corixidae)*

Mechanical Design Methods Lab — Fall 2017

- Collaborated with design team to build and test a small-scale wind turbine through combination of machining and 3D SolidWorks modeling
- Performed contour analysis to suggest additional improvements to prototype

LEADERSHIP & INVOLVEMENT

Member and Volunteer, Monarch THON organization (2016-2019)
Member, Society of Women Engineers (*Penn State Chapter)* (2015-2016)
Member, Penn State SWE Benefitting THON (2015-2016)
Volunteer, Penn State Fresh START (*Students Taking an Active Role Today)* (2015)

SOFTWARE & PROGRAMMING

SolidWorks Engineering Equation Solver Adobe InDesign Adobe Photoshop
MATLAB C++ ArcGIS (ArcMap) MS Office Package

AWARDS

Energy and Environmental Sustainability Laboratory Green Seed Grant